

## THE REFLEX SWITCH: A HIGH-CURRENT, FAST-OPENING VACUUM SWITCH\*

B. Ecker, J. Creedon, L. Demeter, S. Glidden and G. Proulx

Physics International Co.  
2700 Merced Street  
San Leandro, CA 945771. Introduction

The "reflex switch"<sup>1</sup> is a new, ultra-high-power, fast-opening switch suited to pulsed power generation by magnetic energy storage systems. The final, "open" state of the reflex switch can itself serve as a vacuum diode load and generate an intense REB or x-ray pulse; or the opening of the switch can transfer the power pulse to a parallel load.

The basic elements of a magnetic energy storage system using a reflex switch are illustrated in Figure 1. During the "closed" (low-impedance) mode of the reflex switch, the generator builds a current,  $I$ , in the storage inductor,  $L_s$ . When the current is near its peak value the reflex switch makes a very fast transition to its "open" (high-impedance) mode. The sharp increase of series impedance produces a corresponding increase of voltage across the switch, which can be much greater than the generator voltage. The power of the high-voltage output pulse can exceed the input power (the rate of energy accumulation in the inductor during the low-impedance phase) by approximately the ratio of the low-impedance duration to the output pulse duration.

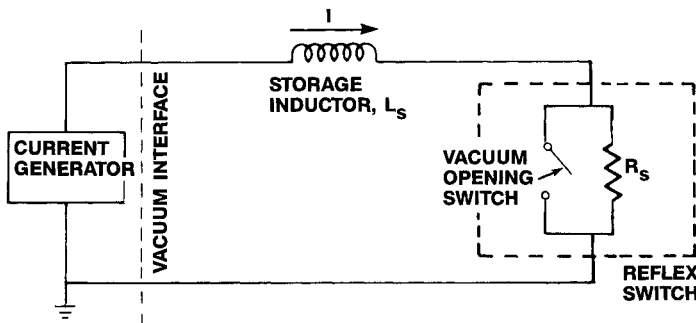


Figure 1. Schematic of a vacuum inductive energy storage system using the reflex switch.

In contrast to other types of high-power opening switches, the reflex switch operates in vacuum. This is a very important property that allows megavolt power pulses to be generated entirely in vacuum, at or near the load, and eliminates the need for the dielectric vacuum interface to insulate the full output voltage of the system. Thus, the basic limitation on power density, caused by dielectric insulator breakdown, is overcome. Instead, it is possible to use the much higher values of power per unit area that can be achieved with magnetic insulation in vacuum. Energy is transported at relatively low power into the vacuum inductive energy store through a low-voltage insulator, and the current in the vacuum

inductor rises over a relatively long period of time. The magnetically stored energy is then converted into a short, high-power output pulse when the switch abruptly opens. The energy density in a vacuum magnetic store can be orders of magnitude greater than is possible for capacitive energy storage, giving magnetic systems great compactness.

2. Reflex Switch Operation

Figure 2 shows the reflex switch configuration used in our experiments. The switch is based on reflex triode physics. It consists of a primary cathode,  $K_1$ , a thin anode,  $A$ , and a secondary cathode,  $K_2$ , which is electrically floating and serves to reflect electrons back through the anode toward  $K_1$ , which in turn repels them back through the anode toward  $K_2$ , etc. The reflexing electrons scatter in the anode and deposit some of their energy in it on each pass. An axial magnetic field is used to minimize radial loss of electrons. Positive ions are accelerated from the anode to the cathode,  $K_1$ .

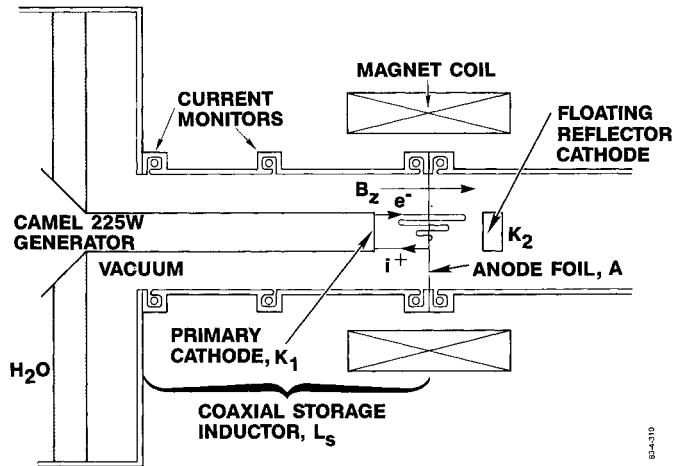


Figure 2. Reflex switch experimental setup.

The combination of multiply reflected electrons and counterstreaming positive ions flowing between cathode,  $K_1$ , and anode,  $A$ , results in several unique properties. One of the most important of these is that the total current in the reflex mode can be orders of magnitude greater than the Langmuir-Child (L-C) current appropriate for an ordinary vacuum diode of the same dimensions. Thus, the "impedance" of the reflex mode can be far lower than the impedance of the  $A$ - $K_1$  gap in the absence of reflexing. The reflex triode can function as a "closed" switch if we first establish the reflex mode and then as an "opening" switch if we bring about an abrupt termination of electron reflexing. This forces a fast transition from the low-impedance reflex mode

\*Work supported by the Defense Nuclear Agency.

# Report Documentation Page

*Form Approved*  
*OMB No. 0704-0188*

Public reporting burden for the collection of information is estimated to average 1 hour per response, including the time for reviewing instructions, searching existing data sources, gathering and maintaining the data needed, and completing and reviewing the collection of information. Send comments regarding this burden estimate or any other aspect of this collection of information, including suggestions for reducing this burden, to Washington Headquarters Services, Directorate for Information Operations and Reports, 1215 Jefferson Davis Highway, Suite 1204, Arlington VA 22202-4302. Respondents should be aware that notwithstanding any other provision of law, no person shall be subject to a penalty for failing to comply with a collection of information if it does not display a currently valid OMB control number.

1. REPORT DATE <b>JUN 1983</b>	2. REPORT TYPE <b>N/A</b>	3. DATES COVERED <b>-</b>			
4. TITLE AND SUBTITLE <b>The Reflex Switch: A High-Current, Fast-Opening Vacuum Switch</b>		5a. CONTRACT NUMBER			
		5b. GRANT NUMBER			
		5c. PROGRAM ELEMENT NUMBER			
6. AUTHOR(S)		5d. PROJECT NUMBER			
		5e. TASK NUMBER			
		5f. WORK UNIT NUMBER			
7. PERFORMING ORGANIZATION NAME(S) AND ADDRESS(ES) <b>Physics International Co. 2700 Merced Street San Leandro, CA 94577</b>		8. PERFORMING ORGANIZATION REPORT NUMBER			
9. SPONSORING/MONITORING AGENCY NAME(S) AND ADDRESS(ES)		10. SPONSOR/MONITOR'S ACRONYM(S)			
		11. SPONSOR/MONITOR'S REPORT NUMBER(S)			
12. DISTRIBUTION/AVAILABILITY STATEMENT <b>Approved for public release, distribution unlimited</b>					
13. SUPPLEMENTARY NOTES <b>See also ADM002371. 2013 IEEE Pulsed Power Conference, Digest of Technical Papers 1976-2013, and Abstracts of the 2013 IEEE International Conference on Plasma Science. Held in San Francisco, CA on 16-21 June 2013. U.S. Government or Federal Purpose Rights License.</b>					
14. ABSTRACT					
15. SUBJECT TERMS					
16. SECURITY CLASSIFICATION OF:			17. LIMITATION OF ABSTRACT	18. NUMBER OF PAGES	19a. NAME OF RESPONSIBLE PERSON
a. REPORT <b>unclassified</b>	b. ABSTRACT <b>unclassified</b>	c. THIS PAGE <b>unclassified</b>	<b>SAR</b>	<b>7</b>	

("closed" switch) to the much higher impedance Langmuir bipolar mode ("open" switch). Reflexing is terminated, in our technique, by allowing the floating electrode,  $K_2$ , to undergo a short-circuit to the anode at the desired time. When the negative potential of  $K_2$  collapses to anode potential, electrons no longer reflect from  $K_2$  and instead deposit in it after one pass through A- $K_1$ . Once reflexing is terminated, the transition of A- $K_1$  to the Langmuir bipolar mode is governed by ion and neutral atom dynamics in A- $K_1$ . These effects play a crucial role in determining the rate at which the impedance of A- $K_1$  increases.

The high-current, reflex triode mode of electron and ion flow was first predicted by Ian Smith from theoretical considerations. Further developments of the theory are given in References 2 and 3. The first experimental observation of the high-current mode was made by Prono *et al.*<sup>2</sup> There is now a considerable amount of experimental evidence indicating that the basic features of the theoretical model are correct. The use of the reflex triode as a switch was first suggested by Creedon.<sup>1</sup>

The potential distribution in the reflex triode, shown in Figure 3, sheds some light on the reason for the high-current mode of operation. Define  $\eta$  as the average number of times an electron encounters the anode prior to stopping in it. In the limit of very low voltage across the A- $K_1$  gap,  $\eta = 1$ , and the potential distribution is that of ordinary Langmuir bipolar flow. The current is about 1.9 times the L-C value. The value of  $\eta$  increases with A- $K_1$  gap potential,  $V$ . For  $\eta > 1$ , the potential distribution is distorted by the space charge of the multiply reflected electrons and the corresponding positive ion flow. The greater the value of  $\eta$ , the greater is this distortion, until  $\eta$  approaches a critical number,  $\eta_c$ , corresponding to a critical gap potential,  $V_R$ . For  $\eta \sim \eta_c$  the potential distribution is relatively flat in most of the A- $K_1$  gap, and most of the potential difference is concentrated in a thin "sheath" near the anode, as shown in Figure 3. This thin sheath becomes the effective diode gap, instead of the much larger A- $K_1$  gap. It is due to this small effective gap that the reflex mode gives very high-current operation relative to ordinary Langmuir bipolar flow.

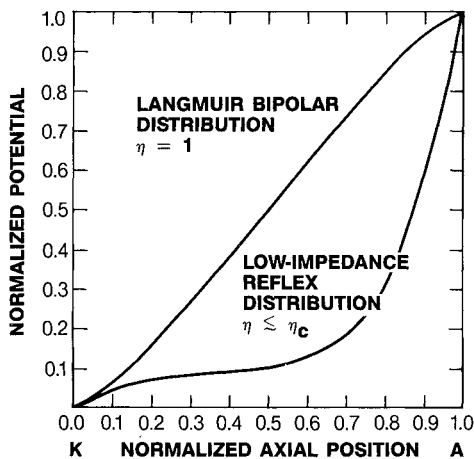


Figure 3. Potential distribution in the reflex mode and in the Langmuir bipolar mode.

As  $V$  approaches  $V_R$  and  $\eta$  approaches  $\eta_c$ , theory predicts that the gap operates essentially as a constant-voltage device with  $V = V_R$  over a large range of current. Figure 4 shows the  $I$  vs.  $V$  characteristic of the A- $K_1$  gap in the reflex mode. The value of  $V_R$  depends on the energy spectrum of reflexing electrons and on the anode thickness. The energy spectrum determines  $\eta_c$  (Reference 2) which in turn determines the  $V_R$  value required to give electrons enough energy to pass through the anode  $\eta_c$  times, at a given anode thickness. For a given electron energy spectrum, increasing the anode thickness raises  $V_R$ . For the reflex triode to serve as a closed switch in a magnetic energy storage system, it is desirable for  $V_R$  to be as low as possible relative to the voltage of the driving power source. This minimizes dissipative losses in the switch and allows maximum current build-up in the storage inductor. We have obtained values of  $V_R$  as low as 15 kV, as compared with the 1-MV power sources that we have used in our studies to date.

As indicated in Figure 4, the external circuit determines the total current in the closed reflex switch, and also the current density, for a

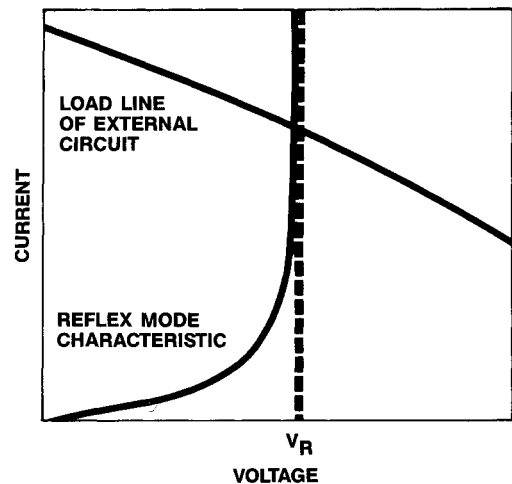


Figure 4. Reflex mode current-voltage characteristic.

given diode geometry. Earlier we indicated that the potential distribution effectively reduces the gap width and allows for high current density. The potential distribution, the current density and  $\eta$  are self-consistently related (along with the electron energy spectrum and the ratio of ion to electron current density).<sup>2</sup> Consequently, the fixing of current density by the external circuit also determines the potential distribution and  $\eta$ . The higher the current density, the smaller the anode sheath with the large potential gradient. This is illustrated in Figure 5, which shows the potential distribution and the value of  $\eta$  at various current densities, for a flat electron energy distribution from zero energy up to full diode potential. This distribution is only one of several energy spectra that we have used for modeling purposes.

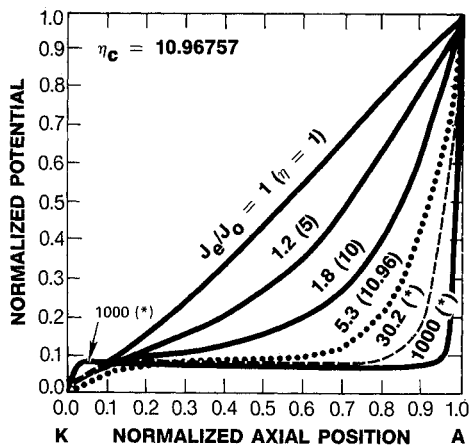


Figure 5. Theoretical potential distribution in the reflex mode at various values of current density and electron transit number,  $\eta$ .  $J_e/J_0$  is the ratio of the electron current density in the reflex mode to the Langmuir-Child electron current density computed using the full A-K spacing. Asterisks indicate values of  $\eta$  that are asymptotically close to  $\eta_c$ .

The operating characteristics of a reflex switch are illustrated in Figure 6. Figure 6a is a plot of switch current versus switch voltage; Figure 6b is a plot of switch voltage versus time. The three lighter curves in Figure 6a represent the characteristics of the device in various modes of operation. The heavy curve in Figure 6a represents the temporal path of switch operation in the current-voltage plane. The curve marked  $I_R$  in Figure 6a represents the low-impedance reflexing mode at the potential  $V_R$ . The curve marked  $I_{BP}$  is the ordinary bipolar mode, with electrons emitted from  $K_1$  and ions from A, but no reflexing electrons. The curve marked  $I_{ER}$  corresponds to the presence of reflexing electrons but no ions. The

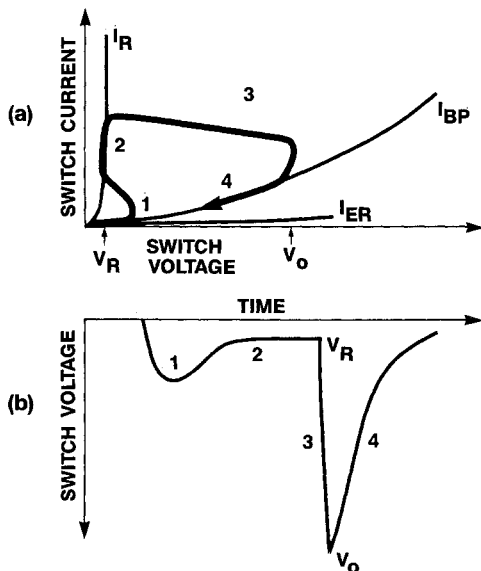


Figure 6. Current and voltage behavior during reflex switch operation. In (a),  $I_R$  is the reflex mode characteristic,  $I_{BP}$  is the Langmuir bipolar mode characteristic, and  $I_{ER}$  is electron-only reflex mode (ionless) characteristic.

time dependence of the switch voltage shown in Figure 6b consists of four phases. These phases are also marked on the heavy curve of Figure 6a. Initially, only reflexing electrons and no ions are present in the A- $K_1$  gap. The switch follows the characteristic curve  $I_{ER}$  and the current is low. When an anode plasma forms, ions begin to flow from the anode. The switch enters Phase 1 which is a transition to the low-impedance mode. In Phase 2, the switch operates on the reflex triode characteristic curve,  $I_R$ , at voltage  $V_R$ . This is the low-impedance, constant-voltage, "closed" mode. When the cathode,  $K_2$  (Figure 2), shorts to the anode, A, the electrons from  $K_1$  stop in  $K_2$  and reflexing ends. The switch enters Phase 3, which is a fast transition from  $I_R$  to the ordinary bipolar characteristic,  $I_{BP}$ . This is the "opening" phase of the switch during which the voltage increases rapidly to a large value,  $V_0$ . In Phase 4 the switch has fully "opened" to the Langmuir bipolar characteristic corresponding to the physical geometry of A- $K_1$ , and the pulse decays along the  $I_{BP}$  curve.

Figure 7 displays representative experimental results obtained using the CAMEL generator (Pulserad 225W) at Physics International Co. The measured voltage across A- $K_1$ , labeled "V-output," shows a reflex switch going through the phases described above. The peak voltage during Phase 1 is 560 kV. The reflexing voltage  $V_R$  in Phase 2 is about 100 kV. The peak open-switch accelerating voltage  $V_0$  in Phase 3 is 1.8 MV. Switch impedance increases at a rate in excess of 1 ohm/ns during

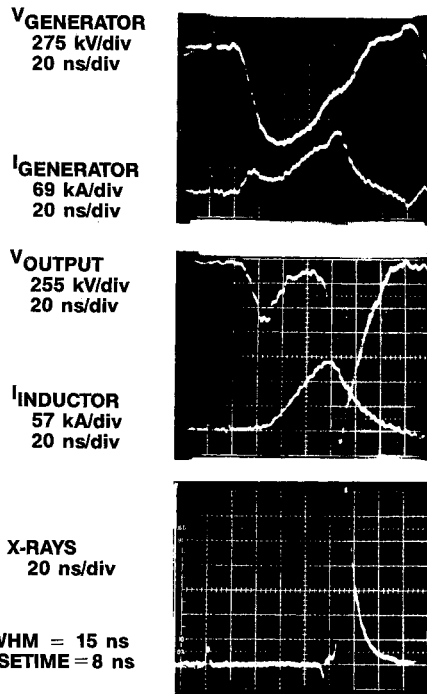


Figure 7. Diagnostic traces of CAMEL Shot No. 5137.

the voltage risetime. The net impedance transition is from 0.8 ohms just prior to switching, to 15.3 ohms at peak voltage, an increase by a factor of 19. The switch current, labeled "I-inductor" in Figure 7, increases to a value of 160 kA during the  $\sim 48$  ns duration of Phase 2, and is 145 kA at the time of peak accelerating voltage. During the

low-impedance phase of the switch, the inductive store accumulates energy at an average rate of 65 GW. The stored energy is released in the output pulse at a peak power of 360 GW. Peak energy in the inductor is 3.4 kJ. The magnetic energy in the store is converted to REB kinetic energy with essentially 100% efficiency. The X-ray pulse occurs at the same time as the high-voltage pulse across the switch and is due to bremsstrahlung from the stopping of the accelerated REB in  $K_2$ . The risetime of the X-ray pulse is 8 ns and the pulse duration is 15 ns (FWHM).

Figure 8 shows a case in which  $K_2$  was withdrawn so that reflexing never terminated. The constant-voltage operation of the reflex mode is well illustrated. (As mentioned in Part 1, the initial transient spike in the voltage waveform represents a delay for anode emission of ions, as required for the low-impedance mode. Preionization of the anode surface may reduce or eliminate the early voltage peak.)

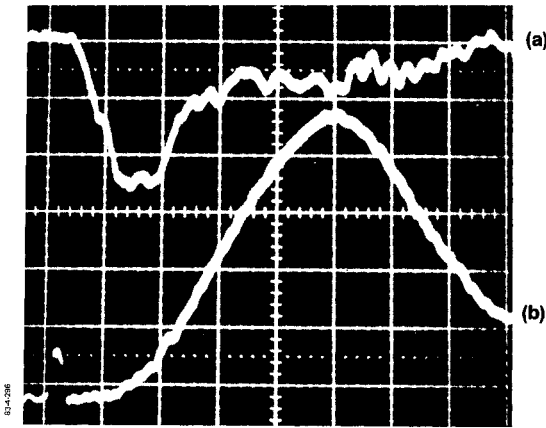


Figure 8. Measured waveforms of reflex switch voltage [(a), 278 kV/div] and current [(b), 32.3 kA/div] with switch kept in "closed," reflex mode for entire pulse. Both waveforms are 20 ns/div.

### 3. Reflex Switch Opening Model

In the previous section we described the basic operation of the reflex switch. Here we focus on our model of the opening of the switch. Analysis of the opening phase of a reflex switch requires the solution of a complex, two-dimensional, time-dependent space-charge-flow program. In addition, the reflex switch represents a highly time-dependent load that is driven, in our studies, by a relativistic electron beam generator. Thus, the generator, storage inductor, and reflex switch must be treated as a coupled, self-consistent system. We have developed a numerical model which treats the problem in that manner, using equivalent circuits.<sup>7</sup> The modeling of the opening reflex switch begins when reflexing electrons are eliminated and the switch begins a transition to the ordinary bipolar mode of operation. However, this transition is quite complex, with several processes occurring simultaneously:

1. Ion emission from the anode decreases dramatically. Ions from the reflexing phase drift out of the A- $K_1$  gap at finite velocity. The much smaller ion current of bipolar flow ensues.

2. Cathode and anode plasmas can expand into the A- $K_1$  gap.
3. Ionizable charge-exchange neutral atoms generated in the anode plasma<sup>8-10</sup> can flow into the A- $K_1$  gap both before and during the opening of the switch.
4. The problem is basically two-dimensional. Fringing electric fields and cathode sheath emissions cause higher current densities at the cathode edge than at the center. In addition, the net magnetic field vector varies with radius, since the ratio of the azimuthal self-field to the axial applied field is a function of radial position.

As a first step in solving this problem we have adopted the following simple model. The sudden termination of electron reflexing causes an abrupt, large reduction in the ion flux emitted from the anode. However, the high-flux ions which were injected before reflexing terminated require a finite time to clear out of the A- $K_1$  gap. The widening gap between the trailing edge of these ions and the anode is the opening switch in our model. The relation between the voltage and current across this gap of width  $x(t)$  is assumed to be that of Langmuir bipolar flow. During the opening phase, it seems likely that the potential of the receding region of high-flux ions does not differ greatly from that of the cathode. Thus, the high-flux ions are not accelerated appreciably and drift out at essentially constant velocity even though the voltage across the widening gap is increasing rapidly. (Note that the potential of the receding high-flux ion region during the opening phase may not be the same as the field-free region of the A- $K_1$  gap during reflexing. Also, preliminary analysis indicates the potential of the receding region, although close to that of the cathode, may not be completely field-free.) If these ideas are correct, the drift velocity of the departing ions,  $v_i$ , is simply the velocity with which they were injected into the field-free region during reflexing. This velocity governs the rate of opening of the switch:

$$\frac{dx}{dt} = v_i = \left( \frac{2q_i \Delta V}{m_i} \right)^{1/2} \quad (1)$$

where  $\Delta V$  is the potential difference between the anode and the field-free region during reflexing ( $\Delta V \leq V_R$ ), and  $q_i$  and  $m_i$  are the charge and mass of the ion, respectively. The value of  $\Delta V$  is governed by the electron energy spectrum in A- $K_1$  during reflexing. The example shown in Figure 5 has  $\Delta V \approx V_R$ ; but the difference in potential between the field-free region and the cathode could be considerably larger for other electron energy distributions than was assumed for Figure 5. In all of the calculations presented here, we have neglected any difference in potential between the field-free region and the cathode, and have set  $\Delta V$  equal to the full reflexing voltage,  $V_R$ . We have also assumed the ions to be singly ionized carbon. As we shall show, these assumptions give calculated results which compare meaningfully with the experimental data. It is possible, however, that assuming smaller  $\Delta V$  and lighter ions (protons) would give equally useful results.

For simplicity, we begin with the initial value  $x = 0$  when reflexing stops and the opening phase begins. As  $x$  increases, the impedance of  $A-K_1$  increases according to the familiar formula for space-charge-limited Langmuir bipolar flow. We include fringing effects in our computation of the voltage and current across the opening Langmuir bipolar gap by defining the effective area of the gap as

$$A = \pi (R_c + \epsilon x)^2 \quad (2)$$

where  $R_c$  is the cathode radius and the term  $\epsilon x$  represents the fringing effects. To estimate the value of  $\epsilon$ , measurements of diode voltage and current were made in an ordinary, nonreflex diode (thick anode) at various A-K spacings. The value of  $\epsilon$  was determined by requiring agreement between these data and the L-C prediction using Eq. (2). This procedure consistently gave  $\epsilon = 0.7$ , which we use in our numerical model.

The theoretical scaling predicted by our inductive storage/reflex switch system model depends in a complex way on many experimental variables. Here we simplify by holding all experimental conditions fixed and varying only the charging voltage of the generator. We assume that the reflex switch is in the "closed" mode for 45 ns and that the reflexing voltage,  $V_R$ , is 150 kV (typical values measured). For these conditions our numerical model calculates the peak open-switch voltage and the simultaneous current for various charging voltages, as shown by the curve labelled "scaling curve" in Figure 9. The other four curves through the origin are computed Langmuir bipolar characteristics ( $I_{BP}$  in Figure 6a) for the diode gaps indicated. With the above assumptions, the switch always has opened to approximately the same gap width (2.5 cm) at the time of peak voltage, so the scaling curve falls along the Langmuir bipolar flow characteristic for this gap. The experimental data in Figure 9 are discussed in the next section.

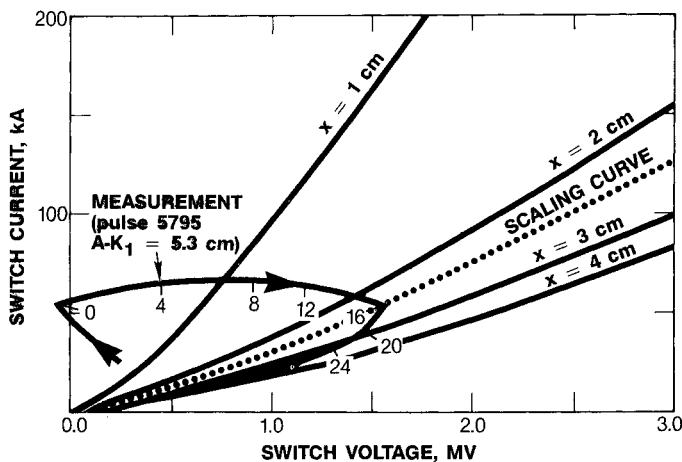


Figure 9. Measured current versus voltage of opening reflex switch with 5.3 cm  $A-K_1$  spacing, with time in ns indicated at hash marks along curve, and  $t=0$  defined at the beginning of switch opening. "Scaling curve" is explained in text. The four curves through the origin are Langmuir bipolar characteristics for the diode gaps ( $x$ ) indicated.

The data presented here were obtained using a vacuum coaxial inductor (Figure 2) with a total vacuum inductance of 275 nH. The reflex switch had dielectric anode, metal  $K_1$  and either dielectric or metal  $K_2$ . The dimensions of  $K_1$ ,  $K_2$ ,  $A-K_1$  and  $A-K_2$  ranged from 1 to 10 cm. Background gas pressure was kept below  $7 \times 10^{-5}$  mmHg in  $A-K_1$  and below  $2 \times 10^{-4}$  mmHg in  $A-K_2$ . The axial magnetic field applied to the reflex switch was typically 15-20 kG. The generator applied a 1-MV, 65-nsec (FWHM) pulse at the input to the storage inductor. The output impedance of the generator was 5.3 ohms. Our experimental studies have documented the dependence of reflex switch performance on all the switch conditions just cited. Not all the observed behaviors are understood as yet. In this paper we restrict our discussion to the major aspects of switch operation.

The measured I-versus-V trajectory shown in Figure 9 (corresponding to Phases 3 and 4 in Figure 6a) was obtained with an  $A-K_1$  spacing of 5.3 cm. The crossing of the Langmuir bipolar characteristics by the measured trajectory shows the opening of the switch (Phase 3). These data are in good agreement with the scaling curve predicted by our numerical model; i.e., the point of peak voltage falls on the scaling curve.

However, at smaller values of  $A-K_1$  spacing, we have observed a considerable discrepancy between the predictions of the model and the experimental results. Figure 10 compares the measured and calculated opening of the switch with an  $A-K_1$  gap of 3.5 cm. The data are from Figure 7 (V-output and I-inductor waveforms). The calculated I-V trajectory reaches the  $I_{BP}$  characteristic for a 3.5 cm gap and follows that characteristic in Phase 4, while the measured trajectory in Phase 4 lies along the  $I_{BP}$  characteristic for a gap of only about 1.5 cm. Thus the data are consistent with the attainment of a well-defined

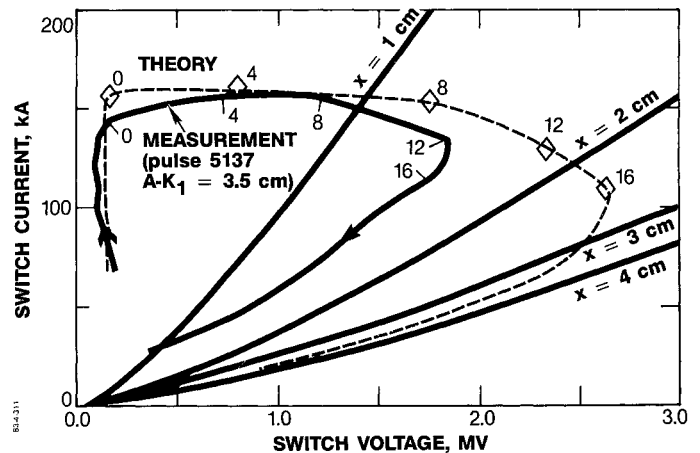


Figure 10. Comparison of calculated and measured curves of current versus voltage of opening reflex switch with 3.5 cm  $A-K_1$  spacing. The measured curve is from the switch voltage and current waveforms shown in Figure 7. Numbers along the curves show time in ns measured from beginning of switch opening. The four curves through the origin are Langmuir bipolar characteristics for the diode gaps indicated.

maximum gap with Langmuir bipolar flow, but indicate an effective final gap width that is appreciably smaller than the A-K<sub>1</sub> spacing, limiting the peak voltage across the switch.

The most plausible explanation for the reduced gap is that not only ions are injected into the A-K<sub>1</sub> gap from the anode plasma during reflexing, but also neutral atoms that subsequently get ionized. As Prono<sup>8</sup> first pointed out, neutrals at  $\lesssim 10$  keV can be created through a charge exchange process between the accelerating ions in the anode sheath and slow neutrals liberated at high densities at the anode surface (by flashover and electron energy deposition). A number of independent observations confirm the influential presence of injected neutral atoms. Greenly<sup>9</sup> has detected neutrals directly. The most obvious influence of neutrals on diode performance is to cause impedance collapse far more rapidly than can be explained in terms of the usual mechanism, i.e., expansion of anode and cathode plasmas.<sup>8,10</sup> It was the observation of anomalously fast diode closure that first prompted Prono to suggest the charge-exchange mechanism.<sup>8</sup> The charge-exchange mechanism implies that the flux of neutrals should be proportional to the ion current density. The effect of neutrals is significant only in diodes that generate a copious flux of ions from the anode, as in the reflex triode.

We do not yet understand how the injected neutrals get ionized in A-K<sub>1</sub> and seem to produce a reduced but approximately constant A-K<sub>1</sub> spacing, as our data suggest (e.g., Figure 10). Perhaps, during reflexing, the region of ionized neutrals effectively extends the anode surface into the gap, just as the receding region of ions during the opening phase extends the K<sub>1</sub> surface into the gap, as shown in Figure 11. Two independent observations in our studies indicate that all during the closed phase of the switch, the region of ionized neutrals moves out from the anode toward K<sub>1</sub> at a velocity of about 40 cm/ $\mu$ sec: (1) the amount of gap closure (as revealed by plotting the data as in Figure 10) divided by the time spent in the low-impedance mode (the time for the closure to occur) consistently gives velocities of 35 to 45 cm/ $\mu$ sec; (2) the full size of the A-K<sub>1</sub> gap divided by the time of final impedance collapse gives velocities of 30 to 35 cm/ $\mu$ sec.

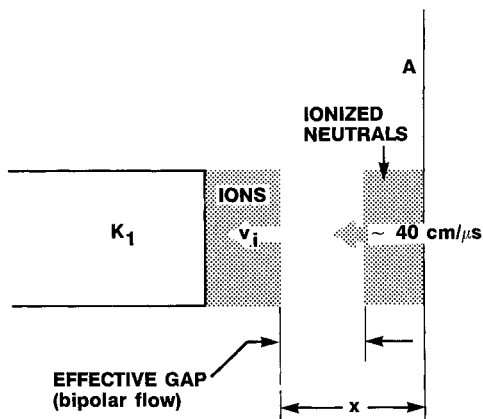


Figure 11. Geometrical model of opening reflex switch.

Obviously, by limiting the opening of the gap, the charge exchange neutrals are detrimental to reflex switch performance. A goal of our present experimental work is to develop a method of circumventing their effect. One possibility is simply to use a larger A-K<sub>1</sub> gap, which would make gap reduction by neutrals relatively less significant. The data of Figure 9 were obtained using a 5.3 cm gap, and the effective maximum gap (as Figure 9 indicates) was about 4 cm. Beyond a certain A-K<sub>1</sub> gap size, the applied electric field becomes too low to properly "light" the anode and cathode for reflexing, and we expect that special techniques for preionizing the anode and cathode become necessary to produce the reflex mode.

#### A-K<sub>2</sub> Operation

In the previous discussion, we assumed that A-K<sub>2</sub> operates in an ideal mode in which (a) electrons reflect elastically from K<sub>2</sub>, and (b) A-K<sub>2</sub> undergoes abrupt impedance collapse, causing abrupt termination of electron reflexing. In practice, we have found that A-K<sub>2</sub> operates in what we term the "reemission mode," which can approach the ideal mode as a limiting case. In the ideal mode, the potential of K<sub>2</sub> is equal either to that of K<sub>1</sub> (causing elastic reflection of electrons) or to that of the anode (preventing reflexing). Several different observations prompted us to consider the possibility that the floating voltage of K<sub>2</sub> can be significantly smaller than that of K<sub>1</sub>, and yet not collapsed to anode (ground) potential either. In such a case, all electrons from K<sub>1</sub> would first strike K<sub>2</sub> (losing energy  $e[V_{K1} - V_{K2}]$  in doing so), and then reemit from K<sub>2</sub>, reimpinging upon the anode and reentering A-K<sub>1</sub> with reduced energy  $eV_{K2}$  (whereas in ideal reflexing, electrons reimpinge upon the anode with no energy loss due to K<sub>2</sub>). The energy reduction of electrons reentering A-K<sub>1</sub> can have important effects on reflex switch operation, explaining the otherwise anomalous observations that initially led us to consider the reemission mode of A-K<sub>2</sub>. These observations include a dependence of  $V_R$  on A-K<sub>2</sub> geometry and a correlation of the optimum K<sub>2</sub> diameter with K<sub>1</sub> diameter. The clearest confirmation of the reemission mode has been our observation of a circular damage pattern in the anode with precisely the diameter of K<sub>2</sub> on a few shots which failed to reflex, suggestive of energetic electron emission from K<sub>2</sub>.

#### References

1. J. Creedon, S. Putnam, I. Smith, U.S. Patent No. 4080549 (1978).
2. D. Prono, J. Creedon, I. Smith and N. Bergstrom, *J. Appl. Phys.* **46**, 3310 (1975).
3. J. Creedon, I. Smith and D. Prono, *Phys. Rev. Letters* **35**, 91 (1975).
4. D. S. Prono, J. W. Shearer, R. J. Briggs, *Phys. Rev. Letters* **37**, 21 (1976).
5. M. S. Di Capua, R. Huff, J. Creedon, *Proc. of the International Topical Conference on Electron Beam Research and Technology*, G. Yonas, editor, Sandia Laboratories, SAND 76-5122, p. 555.
6. D. S. Prono, H. Ishizuka, B. Stallard, W. C. Turner, *Bull. Am. Phys. Soc.* **23**, 903 (1978).

7. J. Creedon, L. Demeter, B. Ecker, G. Proulx, H. Helava, T. Naff, C. Eichenberger, J. Benford, J. Douglas, and T. Young, Physics International Co. Report No. PIFR-2665, December 1982.
8. D. Prono, H. Ishizuka, E. Lee, B. Stallard and W. Turner, J. Appl. Phys. 52, 3004 (1981).
9. J. Greenly and Y. Nakagawa, "Production of Fast Neutrals in Magnetically-Insulated Ion Diodes," Cornell University Laboratory of Plasma Science Report No. LPS-303, October 1982.
10. G. Strobel, "Shorting Time of Magnetically Insulated Reflex Ion Diodes from the Neutral Atom Charge Exchange Mechanism," Lawrence Livermore National Laboratory Report No. UCRL-53199, October 1981.